



## 3D QSAR studies of Salicylanilide benzoates derivatives & generation of new leads as Mycobacterium tuberculosis inhibitors

Prashik B. Dudhe<sup>1,2\*</sup>, Hardik G. Bhatt<sup>2</sup>

<sup>1</sup>Sinhgad College of Pharmacy, Department of Pharmaceutical Chemistry, Vadgaon(Bk), Pune 410041, India.

<sup>2</sup>Institute of Pharmacy, Nirma University. G. Highway, Ahmedabad-382481, India.

**Abstract** : Tuberculosis is one of the tenth primary cause of death throughout the world. The increasing number of drug resistance TB cases day by day and the patient poor compliance for the prolong treatment crating a alarming situation. The best tool to create the lead compounds for any disease is can only be achieved through the Combination of ligand and structure-based approaches. We have carried out comparative molecular field analysis(CoMFA) and comparative molecular similarity indices analysis (CoMSIA) on the reported series of Salicylanilide 4-(trifluoromethyl)benzoates&2-hydroxy-N-phenylbenzamides derivatives as Mycobacterium tuberculosis inhibitors. In CoMFA model, the cross validated  $q^2$  and the non-cross validated  $r^2$  value for training set were found as 0.643 and 0.945, respectively; while in CoMSIA model,  $q^2$  value was 0.819 and  $r^2$  value was 0.954. The generated contour maps (CoMFA & CoMSIA) fields were used for the design of 35 novel 2 & 3-(4-aminobenzamido) benzoic acid derivatives and the prediction the pMIC of the design series were carried out. The series is also checked for the toxicity using osiris property explorer which could be explored in future to identify novel Mycobacterium tuberculosis inhibitors.

**Keywords** : 3D QSAR, CoMFA, CoMSIA, Salicylanilide Benzoates, Mycobacterium Tuberculosis.

### 1.Introduction

*Mycobacterium tuberculosis* is a bacterium responsible for causing tuberculosis (TB) infection all around the globe. It is a tenth primary cause of death throughout the world of human. As per WHO it is considered as a global threat [Deaths= 1.3 million (HIV<sup>-</sup>), 300 000 (HIV<sup>+</sup>) and Infection=10 million, 558000 new resistance cases in 2017].<sup>1</sup> The study data of disease transmission, wellbeing and financial reality of drug-sensitive tuberculosis, an expanding drug-resistance particularly multidrug and extensively drug-resistant tuberculosis (MDR- and XDR-TB), an incident of TB with HIV-contamination, warrant an unquestionable requirement for new drugs.<sup>2</sup>

Recognition of new and one of a kind pathway that are basic for the bacterial development and resistance mechanism to give extrafocuses for the rational designand advancement of novel treatments.

Salicylanilide derivatives have revealed a significant antimycobacterial, antitubercular activity towards drug-sensitive, drug-resistant strains. Additionally, salicylanilides have exhibited the inhibition of some bacterial enzymes for example, transglycosylases from *Staphylococcus aureus* and *Escherichia coli*<sup>3-5</sup>

Thus with the aim to design novel Anti-TB inhibitors which can overcome the problem of resistance. We have carried out comparative molecular field analysis (CoMFA) and comparative molecular similarity indices analysis (CoMSIA) on the reported series of Salicylanilide 4-(trifluoromethyl)benzoates & 2-hydroxy-N-phenylbenzamid derivatives as Mycobacterium tuberculosis inhibitors. The generated contour maps (CoMFA & CoMSIA) fields were used for the design of 35 novel 2 & 3-(4-aminobenzamido) benzoic acid derivatives and also predicting the activity (pMIC) of the series. The series is also checked for the toxicity using osiris property explorer.<sup>6-15</sup>

## 2. Materials and Methods

### 2.1. Dataset

We selected the set of 37 Anti-TB inhibitors from literature<sup>3& 5</sup>. The structures and activity study data are shown in Table 1. In the present study, the negative log of minimum Inhibitory concentration (pMIC) value was used as the dependent variable in the 3D-QSAR study. The 3D-structures of the molecules were drawn using the *Builder* module of Sybyl. Energy minimization of the ligands was carried out using the Powel gradient method, the Tripos force field, Gasteiger Hückel charges and a distance dependent dielectric, till a gradient of  $0.01 \text{ kcal mol}^{-1} \text{ \AA}^{-1}$  was achieved.

The set of molecules was divided into training set (24 molecules) for the generation of QSAR model and test set (06 molecules) for validating models. The outliers (07 molecules) were removed for creating the better model. The test set molecules was selected in such a way, that it should be a representative of the entire series and also have a similar activity ranges similar to training set.<sup>16-17</sup>

### 2.2. Computational details

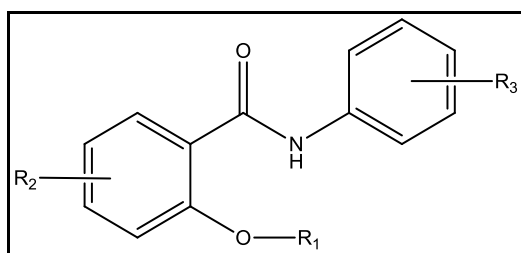
The study was performed using molecular modelling package Sybyl-X (v2.0, Tripos Inc., USA) installed in a machine running on a 2.10 GHz Intel core2 duo processor with 2GB RAM and 500 GB hard disk with windows 7 ultimate as an operating system.

### 2.3. Alignment

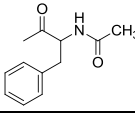
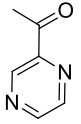
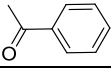
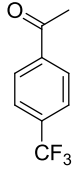
#### Distill

Mol2 database of the series was subjected to rigid body alignment using maximum common substructure (MCS) defined by Distill. All the Compounds were aligned to the compound no1 as it contains an atoms common backbone or common core of all the structures used for the alignment.

**Table 1: Structures, experimental and predicted inhibitory activities along with residuals of salicylanilide 4-(trifluoromethyl)benzoates & 2-hydroxy-N-phenylbenzamid derivatives.**



**Figure 1: salicylanilide 4-(trifluoromethyl)benzoates & 2-hydroxy-N-phenylbenzamid score scaffold**

Comp. No.	R <sub>1</sub>	R <sub>2</sub>	R <sub>3</sub>	pMIC*	pMIC Predicated			
					COMFA	Residule	COMSIA	Residule
1	H	H	H	0.531	0.542	-0.011	0.531	0.000
3	H	5-Cl	3,4-diCl	1.597	1.605	-0.008	1.612	-0.015
5		4-Cl	4-CF <sub>3</sub>	3.004	2.958	0.046	2.958	0.046
6		4-Cl	3,4-DiCl	2.704	2.729	-0.025	2.706	-0.002
7		4-Br	4-CF <sub>3</sub>	3.041	3.010	0.031	3.030	0.011
8		4-Cl	4-CF <sub>3</sub>	2.625	2.662	-0.037	2.683	-0.058
9		4-Cl	3,4-diCl	2.626	2.531	0.095	2.619	0.007
11		4-Cl	3-CF <sub>3</sub>	2.324	2.419	-0.095	2.361	-0.037
12		4-Cl	3-Br	2.335	2.239	0.096	2.199	0.136
13#		5-Cl	4-CF <sub>3</sub>	2.625	2.658	-0.033	2.636	-0.011
14		4-Cl	4-CF <sub>3</sub>	2.623	2.685	-0.062	2.685	-0.062
15		4-Cl	3,4-diCl	2.624	2.615	0.009	2.660	-0.036
16		4-Br	4-CF <sub>3</sub>	2.667	2.669	-0.002	2.669	-0.002
20		4-Cl	3-Cl	2.055	2.126	-0.071	2.109	-0.054
21		5-Cl	3-Cl	2.055	1.967	0.088	2.051	0.004
22		4-Cl	4-Cl	2.356	2.101	0.255	2.196	0.160
23#		5-Cl	4-Cl	2.055	2.101	-0.046	2.196	-0.141
24		4-Cl	3,4-diCl	2.689	2.598	0.091	2.577	0.112
25		5-Cl	3,4-diCl	2.388	2.575	-0.187	2.569	-0.181
26		4-Cl	3-Br	2.397	2.323	0.074	2.266	0.131
27		5-Cl	3-Br	1.795	2.116	-0.321	2.116	-0.321
28		4-Cl	4-Br	2.356	2.200	0.156	2.200	0.156
29#		5-Cl	4-Br	2.096	2.122	-0.026	2.122	-0.026
30#		4-Cl	3-F	1.738	1.914	-0.176	1.825	-0.087
31		5-Cl	3-F	2.039	1.940	0.099	1.980	0.059
32#		4-Cl	4-F	1.738	1.819	-0.081	1.755	-0.017
34		4-Cl	4-CF <sub>3</sub>	2.688	2.533	0.155	2.537	0.151
35		5-Cl	4-CF <sub>3</sub>	2.387	2.528	-0.141	2.473	-0.086
36#		4-Cl	3-CF <sub>3</sub>	2.387	2.496	-0.109	2.448	-0.061
37		4-Br	4-CF <sub>3</sub>	2.726	2.702	0.024	2.713	0.013

pMIC\*- Experimental minimum Inhibitory concentration

#Test set Molecules

## 2.4. Statistical analysis

The CoMFA and CoMSIA model generated through PLS (**Partial least squares**) regression analysis. PLS analysis was carried out by two methods the leave-one-out (LOO) and cross-validation (CV) for generating the 3DQSAR analysis, The above two methods generate  $q^2$  and  $r^2_{cv}$ , respectively, which is nothing but the statistical index of predictive power. The evaluation of the non-cross validated models were done by conventional correlation coefficient ( $r^2$ ), standard error of estimation (SEE) and F values. The derived models were checked for the statistical certainty by the 100-cycle bootstrap. Which produced the bootstrap  $r^2(r^2_{boot})$  [mean correlation coefficient]. The PLS analysis run again without validation considering the most favourable number of components to create CoMFA and CoMSIA.<sup>18</sup> The test set molecules (06 compounds) are the only molecules involved in calculating the predictive  $r^2$  ( $r^2_{pred}$ ) and has a formula i.e.  $r^2_{pred} = SD - PRESS / SD$  where, SD is the sum of the squared deviations between the inhibitory activity of the test set molecules and the mean inhibitory activity of a training set molecules, and PRESS is the sum of squared deviations between predicted and actual activity values for every molecule in a test set. The training set was initially checked and removed 07 Molecules as outliers because its residual value between experimental pMIC and predicted pMIC values is greater than 1.

### 3. Results and Discussion

The best 3D-QSAR model was selected from the various numbers of Runs. The one with the acceptable statistical parameter was selected and are given in following Table 2.

#### 3.1.CoMFA analysis

The generated CoMFA model consists of the cross-validated correlation coefficient  $q^2$  of 0.643 with six components. The non cross-validated PLS analysis produced a correlation coefficient ( $r^2$ ) of 0.945, cross-validated a correlation coefficient ( $r^2_{cv}$ ) 0.689. F value of 67.968 and an estimated standard error (SE) of 0.120. The steric field descriptors explain 84.85% of the variance, while the electrostatic descriptors explain 15.15% of the variance, signifying that the contribution of the steric field is dominant. The model was checked for its robustness the bootstrap analysis. The bootstrap analysis gave a correlation coefficient ( $r^2_{bs}$ ) of 0.983 which supports the statistical validity of the derived CoMFA model.

#### 3.2.CoMSIA analysis

The CoMSIA analysis was also generated using the above mentioned aligned test and training set. The results were obtained by using combination of steric, electrostatic, hydrophobic, H-bond donor and acceptor fields and their field contributions were 0.04 % 0.07%, 0.56%, 0.31% & 0.02 % respectively. Combination of these fields yielded  $aq^2$  value of 0.814 with six components, non cross validated  $r^2_{ncv}$  of 0.954 having standard error of prediction of 0.123,  $r^2_{cv}$  has a value of 0.651. F value as 64.922 with bootstrap  $r^2_{bs}$  value of 0.976. Steric, electrostatic Hydrogen bond acceptor contributions were found to be poor.

**Table 2 Statistical Data**

PLS Statistics	CoMFA	CoMSIA
N	6	6
$q^2$	0.643	0.819
$r^2_{cv}$	0.689	0.651
$r^2$	0.971	0.957
$r^2_{pred}$	0.874	0.733
$r^2_{bs}$	0.983	0.976
F	67.968	64.922
SE	0.120	0.123
PLS Components	6	6
Field Contribution		
Steric	0.849	0.04
Electrostatic	0.152	0.07
Hydrophobic	--	0.56
H-bond donor	--	0.31
H-bond acceptor	--	0.02

$q^2$  is the leave one out (LOO) validation coefficient;  $r^2_{ncv}$  is the non-cross validation coefficient;  $r^2_{cv}$  is the cross-validation coefficient;  $r^2_{bs}$  is the bootstrapping coefficient; N is the optimal number of components (PLS components); F test is the Fischer-test value; SEE is the standard error of estimation;  $r^2_{pred}$  is the predictive correlation coefficient.

#### 3.3.Validation of CoMFA and CoMSIA Models

While developing the 3D-QSAR models test set molecules were excluded. The predictive QSAR model is validated through the external validation. The predicted pMIC values were found to be in good accordance with the experimental outputs within statistically tolerable limits. The predictive correlation coefficient  $r^2_{pred}$  for CoMFA and CoMSIA models derived was 0.874 & 0.733 respectively. The graphical representation is shown in the Fig. 3A & B for predicted pMIC versus experimental pMIC for CoMFA and CoMSIA model. We cannot really only on the  $r^2_{pred}$  for the predictive property of a model it was done with modified  $r^2$  as  $r^2_m$ ,  $R^2$  &  $R_0^2$  are squared correlation coefficient values between observed and predicted values of the test set compounds with

intercept and without intercept respectively. The  $R^2$ ,  $R_0^2$  and  $k$  values obtained from the graph are shown in Fig. 3A & B. The other required circumstance for a model to be considered as dependable predictive model was stated by Golbraikh and Tropsha and are given in Table 3 together with testset results of CoMFA and CoMSIA model.

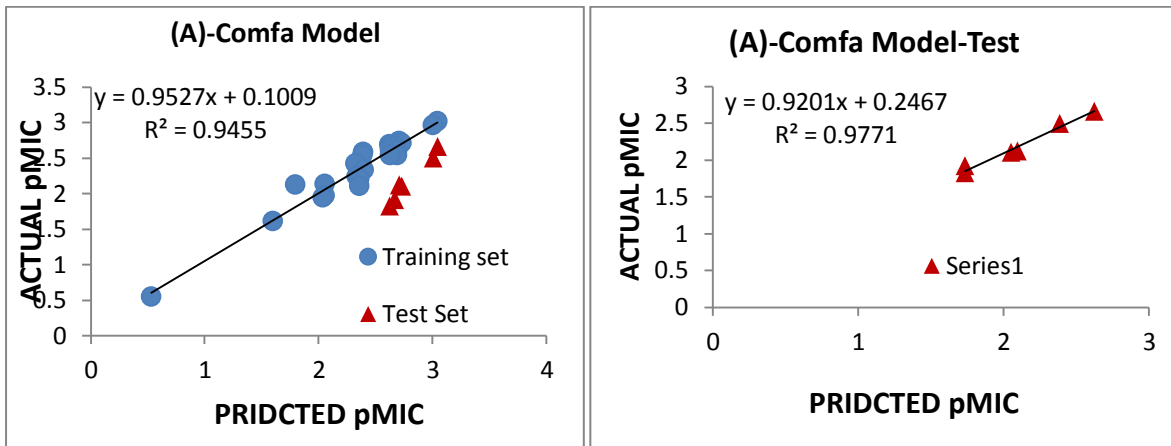


Fig. 3.A Linear regression analysis graph for CoMFA model

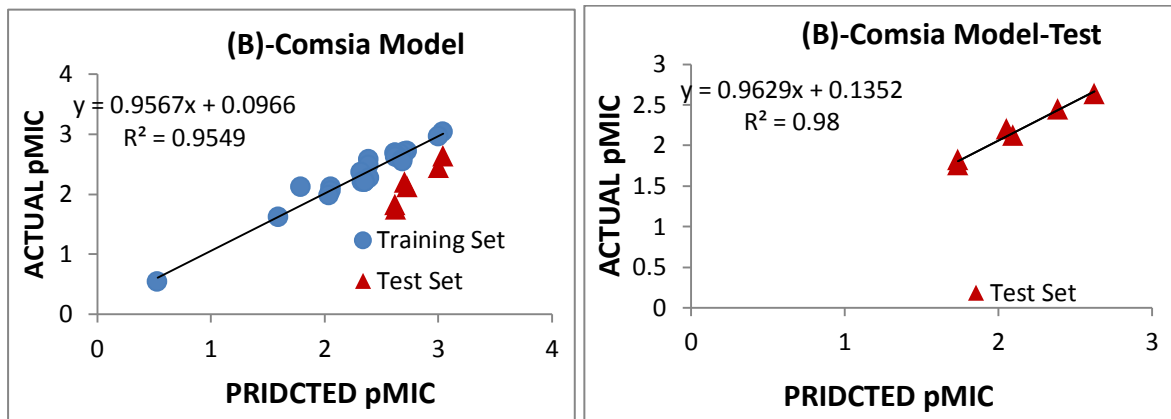


Fig. 3.B Linear regression analysis graph for CoMSIA model

Table 3. Parameters for model validation.

Sr. No.	Parameters	Value for a model to have good predictive power	Test Results	
			CoMFA	CoMSIA
1.	$q^2$	$>0.5$	0.643	0.819
2.	$R^2$	$>0.6$	0.945	0.954
3.	$R_0^2$	Close to the value of $R^2$	0.977	0.980
4.	$(R^2 - R_0^2 / R^2)$	$<0.1$	-0.03386	-0.02725
5.	$R^2_m = R^2 * (1 - \sqrt{R^2 - R_0^2})$	$>0.5$	0.94962	0.95712

### 3.4. CoMFA contour maps analysis

In CoMFA steric contour map, the sterically favourable and sterically negative areas are denoted by green and yellow contours, respectively. While in CoMFA electrostatic contour maps, electropositive charge favourable and electronegative charge favourable regions are represented by blue and red contours respectively. The sterically favourable bulky group in the green region of  $R_3$  substituent's will contribute for increasing the inhibitory activity shown in figure 4(A). The justification for the above can be seen by comparing the pMIC of compound 1 ( $R_3=H$ ) and 5 ( $R_3=4CF_3$ ) (pMIC=0.531 & 3.004) respectively. Steric unfavourable yellow contour near  $R_1$  region. This could be verified by matching the pMIC of compounds 7 & 37 (pMIC=3.041 & 2.726) respectively.

The electrostatic contour map of CoMFA model (Fig. 4(B)); a blue contour (electropositive) was present at nitrogen amide bond, on C-3 position of Phenyl ring and on the C-2 position of  $R_1$  substituent's Phenyl group. All the above mentioned groups favourable at this position. Hence compound 09 ( $R_1 =$  Pyrazine, pMIC = 2.626) showed more potency as compared to compounds 1 & 3 ( $R_1 = H$ , pMIC=0.531, 1.597).

The red contour map (electronegative) (Fig. 4(B)) near carbonyl group of amide linkage and  $CF_3$  group on *para* position of both the phenyl moieties ( $R_1$  &  $R_2$ ) were found to be favourable at these positions. It can be clearly observed with the compound 13 ( $R_1=$ Pyrazine &  $R_2=p-CF_3$ , pMIC = 2.625) were more potent than non substituted derivatives (Compound 3, pMIC = 1.597) at  $R_1$  &  $R_2$  positions.

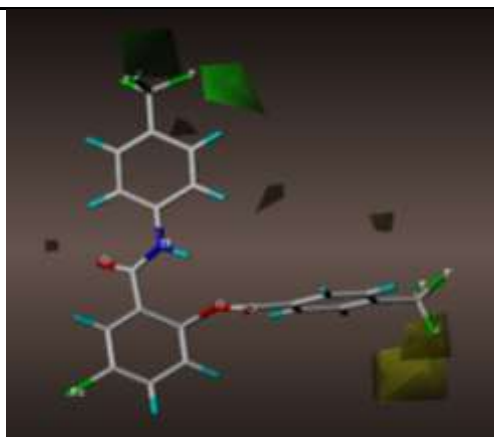


**Fig. 4 A: CoMFA Steric Contour Map Favourable (green) and unfavourable (yellow)**

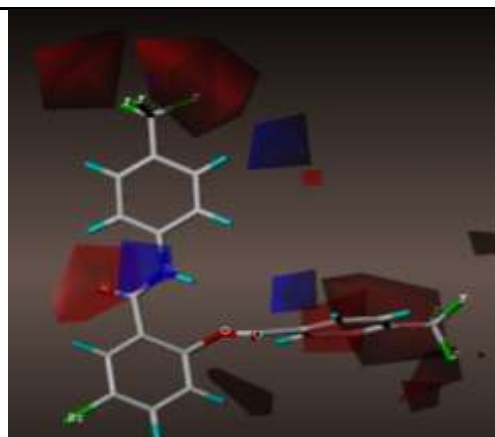


**Fig. 4 B: CoMFA Electrostatic Contour Map Electropositive (blue) and electronegative (red) fields**

### 3.5. CoMSIA contour maps analysis

Same as that of the CoMFA contour map CoMSIA contour map also calculates both steric and electrostatic fields but uses hydrophobic, HBD and HBA fields with the fixed levels of 80 and 20% for Favoured and disfavoured regions. The hydrophobic region in Fig. 5A is shown by yellow- favoured hydrophobic region (80% contribution) and gray- hydrophilic region (20% contribution). The only one big yellow colour contour covering the hydrophobic favoured  $CF_3$  on *para* position of the aniline moiety was responsible for the increasing the pMIC value. This can be observed by comparing the pMIC value of compound 11 ( $R_3=p-CF_3$ , pMIC = 2.324) & compound 21 ( $R_3=3-Cl$ , pMIC = 2.055). Two hydrophobic unfavoured gray contour maps were aniline moiety and 2, 3, 4 & 5 position of the salicylic group revealed the need of the hydrophilic groups in the above region to increase the pMIC. Hydrophobic fields made largest contribution to CoMSIA model.

The graphical explanation of the HBD interactions in the CoMSIA model is shown in Fig. 5B. Cyan colored contours (HBD: favoured) (80% contribution) and purple colored contours (HBD: unfavoured) (20% contribution) Table 2 showed that HBD made second largest contribution to CoMSIA model. Two cyan colored areas were observed near the amide group and near the phenyl ring of  $R_1$  which is necessary for the activity. A purple polyhedron near the carbonyl group of the ester linkage is indicative of a disfavoured HBD region.

The graphical explanation of the HBA interactions in the CoMSIA model is shown in Fig. 5C. Magenta colored contours (HBA: favoured) and red contours (HBA: unfavoured). A large magenta contour was present near the carbonyl oxygen of ester linkage. Carbonyl oxygen is a H-bond acceptor which attacks on a protons, showed a favourable interaction of HBA group in this region for increasing the pMIC value. The red colored contour was found out away from the molecular area and shown that there is no HBA in this region.

Analysis of CoMFA and CoMSIA contour plots put enough light on the series to understand the binding mode interaction between the inhibitors and binding site of Anti-TB enzyme.

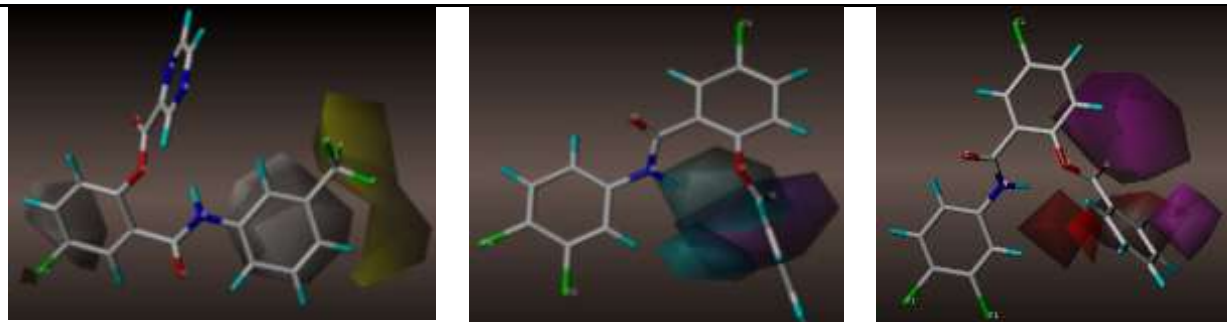


**Fig. 5 A: CoMSIA hydrophobic Contour Map Favourable (yellow) and unfavourable (grey)**

**Fig. 5 B: CoMSIA hydrogen bond donor Contour Map Favourable (cyan) and unfavourable (purple)**

**Fig. 5 C: CoMSIA hydrogen bond acceptor Contour Map. Favourable (magenta) and unfavourable (red)**

#### 4.Generation and prediction of pMIC of new leads

With the help of the generated 3D QSAR analysis and the generated contour maps in 3D QSAR study. We have designed a total of 35 novel 2 & 3-(4-aminobenzamido) benzoic acid derivatives as MTB inhibitors for treatment of tuberculosis and Prediction of the pMIC values of the generated leads were also calculated. (Table 4) using both the (CoMFA and CoMSIA) models. The predicted values of the lead series were found to be in a similar range as that of the studied QSAR series.

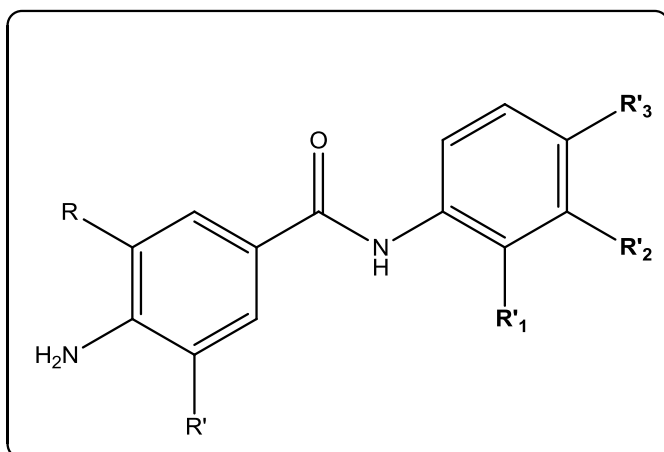
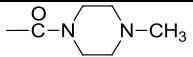
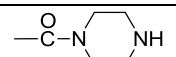
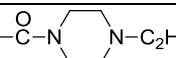
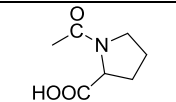
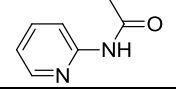
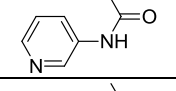
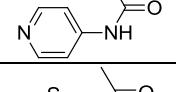
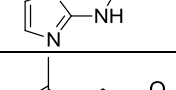
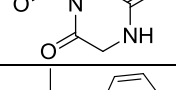
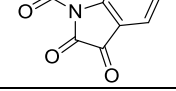
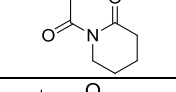
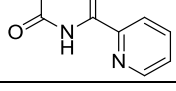
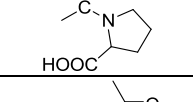
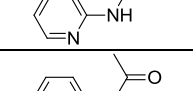
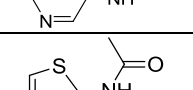
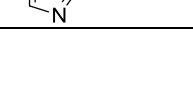
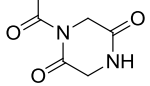
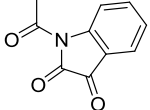
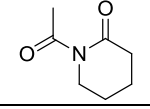
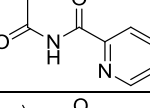
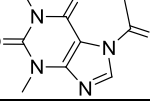
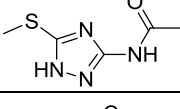
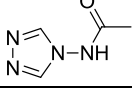
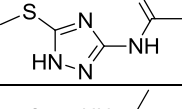
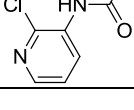
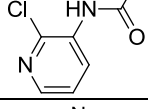
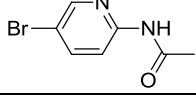
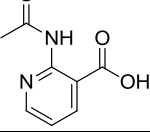
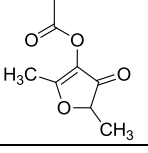
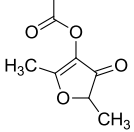


Table 4. Structure of designed compounds with predicted activity

Sr. No.	Comp. Code	R	R'	R'1	R'2	R'3	Predicted	
							pMIC CoMFA	pMIC CoMSIA
1.	D-5	H	H	-COOC <sub>2</sub> H <sub>5</sub>	H	H	1.064	2.1
2.	D-6	H	H	-COOC <sub>3</sub> H <sub>7</sub>	H	H	0.867	2.084
3.	D-9	H	H	-COOC <sub>4</sub> H <sub>9</sub>	H	H	1.317	2.046
4.	D-8	H	H		H	H	1.196	2.04
5.	D-10	H	H	H		H	1.365	2.151
6.	D-16	H	H	H	Cl	F	0.998	2.044
7.	D-22	H	H		H	H	1.21	2.106
8.	D-23	H	H		H	H	1.225	2.119
9.	DX-1	H	H		H	H	1.358	2.365
10.	DX-3	H	H		H	H	1.063	2.008
11.	DX-5	H	H		H	H	1.065	2.092
12.	DX-7	H	H		H	H	1.228	2.078
13.	DX-9	H	H		H	H	1.191	2.166
14.	DX-12	H	H		H	H	1.11	2.18
15.	DX-14	H	H		H	H	1.38	2.183
16.	DX-18	H	H		H	H	1.289	2.081
17.	DX-20	H	H		H	H	1.117	2.151
18.	DX-26	H	H	H		H	0.986	2.156
19.	DX-27	H	H	H		H	1.265	2.154
20.	DX-28	H	H	H		H	1.233	2.155
21.	DX-29	H	H	H		H	1.13	2.153

22.	DX-30	H	H	H		H	0.698	2.151
23.	DX-31	H	H	H		H	1.525	2.211
24.	DX-33	H	H	H		H	1.799	2.041
25.	DX-34	H	H	H		H	1.255	2.155
26.	DX-35	H	H	H		H	1.796	2.308
27.	DY-2	H	H		H	H	1.443	2.313
28.	DY-6	H	H		H	H	1.387	2.264
29.	DY-9	H	H	H		H	1.091	2.235
30.	DY-11	H	H	H		H	1.138	2.155
31.	DY-12	H	H		H	H	1.313	2.11
32.	DY-18	H	H		H	H	1.093	2.059
33.	DY-15	H	H	H		H	1.506	2.154
34.	DY-23	H	H		H	H	1.803	2.307
35.	DY-24	H	H	H		H	2.031	2.306

## General structure of 2 & 3-(4-aminobenzamido) benzoic acid derivatives

### 5. Toxicity prediction study

The designed new leads series of 35 compounds were also subjected to the *in silico* toxicity risk prediction study using osiris property explorer, which uses Chou and Jurs algorithm, Factors of toxicity risk management depends on a computed set of structural fragment that give rise to toxicity alerts in case they are present in the structure. Factors like mutagenicity, tumorigenicity, irritant and reproductive effects were predicted in the study. Results of toxicity prediction (Table 5) revealed that only one compound (D9) is at risk while remaining all the compounds passes the criteria of toxicity.

**Table 5. Toxicity Prediction Study**

Comp. Code	Mutagenic	Tumorigenic	Irritant	Reproductive effective	cLogP	Solubility	Drug likeness	Drug Score
D-5	No	No	Medium	No	2.45	-3.64	-2.37	0.36
D-6	No	No	No	Medium	2.9	-3.91	2.59	0.61
D-8	No	No	No	No	1.91	-2.42	9.39	0.88
D-9	No	No	High	No	3.36	-4.18	-2.14	0.2
D-10	No	No	No	No	1.91	-2.42	7.86	0.88
D-16	No	No	No	No	2.84	-4.25	-1.76	0.44
D-22	No	No	No	No	1.66	-2.78	5.36	0.88
D-23	No	No	No	No	2.83	-3.04	5.3	0.82
DX-1	No	No	No	No	1.67	-3.39	4.06	0.83
DX-3	No	No	No	No	2.63	-4.46	3.21	0.72
DX-5	No	No	No	No	2.28	-3.92	2.71	0.77
DX-7	No	No	No	No	2.28	-3.92	2.32	0.76
DX-9	No	No	No	No	2.9	-4.45	3.34	0.71
DX-12	No	No	No	No	0.53	-2.47	5.04	0.88
DX-14	No	No	No	No	2.55	-5.2	0.59	0.51
DX-18	No	No	No	No	2.4	-3.78	0.89	0.69
DX-20	No	No	No	No	2.12	-3.89	3.18	0.77
DX-26	No	No	No	No	1.67	-3.39	2.42	0.8
DX-27	No	No	No	No	2.63	-4.46	1.44	0.67
DX-28	No	No	No	No	2.28	-3.92	0.91	0.68
DX-29	No	No	No	No	2.9	-4.45	1.57	0.66
DX-30	No	No	No	No	0.53	-2.74	3.35	0.86
DX-31	No	No	No	No	2.55	-5.2	0.5	0.43
DX-33	No	No	No	No	2.4	-3.78	-0.79	0.53
DX-34	No	No	No	No	2.12	-3.89	1.41	0.71
DX-35	No	No	No	No	2.05	-5.22	2.86	0.59
DY-2	No	No	No	No	2.14	-4.55	4.38	0.57
DY-6	No	No	No	No	1.14	-5.74	5.11	0.62
DY-9	No	No	No	No	1.6	-4.81	0.24	0.44
DY-11	No	No	No	No	2.98	-4.42	0.73	0.59
DY-12	No	No	No	No	2.98	-4.42	2.54	0.68
DY-18	No	No	No	No	3.35	-5.28	0.58	0.47
DY-15	No	No	No	No	2.11	-4.46	1.4	0.65
DY-23	No	No	No	No	2.46	-4.6	2.21	0.67
DY-24	No	No	No	No	2.46	-4.6	0.17	0.54

### 6. Conclusion

The generated 3D QSAR models show good validity and consistency and used it for the designing of novel inhibitors to treat tuberculosis and also used for the prediction of pMIC activity of designed compounds.

All the toxicities were found to be in acceptable limits, Hence, it was concluded here that by a combination of the in silico methods we can design a new series, which may be a good lead to develop novel inhibitors for treatment of tuberculosis.

## 6. Acknowledgement

The authors gratefully acknowledge the contributions of Professor M.N. Navale, President and Dr. (Mrs.) S.M. Navale, Secretary, Sinhgad Technical Education Society, Pune, for constant motivation and encouragement and also thankful to Nirma University, Ahmedabad, India for providing necessary facilities.

## 7. References

1. World Health Organization, Tuberculosis (TB), 2018.
2. Ducati RG, Ruffino-Netto A, Basso LA, Santos DS. The resumption of consumption. A review on tuberculosis. *Mem Inst Oswaldo Cruz* 2006;101:697e714.
3. Krátký M, Vinsová J, Buchta V, Horvati K, Bösze S, Stolaríková J. New amino acid esters of salicylanilides active against MDR-TB and other microbes. *Eur J Med Chem* 2010;45:6106e13
4. Waisser K, Bures O, Holy P, Kunes J, Oswald R, Jiraskova L, Pour M, Klimesova V, Kubicova L, Kaustova J. Relationship between the structure and antimycobacterial activity of substituted salicylanilides. *Arch Pharm* 2003;336:53e71.
5. Krátký M, Vinsová J. Salicylanilide ester prodrugs as potential antimicrobial agents a review. *Curr Pharm Des* 2011;17:3494e505.
6. Mali RK, Somani RR, Toraskar MP, Mali KK, Naik PP, Shirodkar PY. Synthesis of some antifungal and anti-tubercular 1, 2, 4-triazole analogues. *Int. J. Chem. Tech. Res.* 2009 Apr;1:168-73.
7. Arya V. A review on anti-tubercular plants. *Int J Phar Tech Res.* 2011;3:872-80.
8. Pawar PY, Bhise SB, Rindhe SS, Mane RA. Synthesis of substituted sulphaquinoxalinones as antimycobacterium tuberculosis agents. *Int J Pharm Tech Res.* 2009;1(2):252-5.
9. Pandey A, Rajavel R, Chandraker S, Dash D. Synthesis of Schiff bases of 2-amino-5-aryl-1, 3, 4-thiadiazole and its analgesic, anti-inflammatory and anti-bacterial activity. *Journal of Chemistry.* 2012 May 3;9(4):2524-31.
10. Visagaperumal D, Kumar RJ, Vijayaraj R, Anbalagan N. Microwave-induced synthesis of some new 3-substituted-1, 3-thiazolidin-4-ones for their potent antimicrobial and antitubercular activities. *Int. J. Chem. Tech. Res.* 2009;4:1048-51.
11. Somani RR, Balkund VD, Nikam SR, Shirodkar PY, Zope DB. Synthesis, antibacterial and anti-tubercular evaluation of some 1, 3, 4-oxadiazole based Mannich bases. *International Journal of ChemTech Research.* 2013 Jul;5(5):2588-92.
12. Prajapati K, Singh S, Pathak AK, Mehta P. QSAR analysis on some 8-methoxy quinoline derivatives as H37RV (MTB) inhibitors. *Int J ChemTech Res.* 2011;3(1):408-22.
13. Arunkumar S, Ilango K, Manikandan RS, Sudha M, Ramalakshmi N. Synthesis, Characterisation and Biological Evaluation of some novel 2, 5-Disubstituted-1, 3, 4-oxadiazole derivatives of Gallic acid. *International Journal of Chem Tech.* 2009;1:1094-9.
14. Dewangan D, Pandey A, Sivakumar T, Rajavel R, Dubey RD. Synthesis of some novel 2, 5-disubstituted 1, 3, 4-oxadiazole and its analgesic, anti-inflammatory, anti-bacterial and anti-tubercular activity. *Int. J. Chem. Tech. Res.* 2010 Jul;2(3):1397-412.
15. Humaedi A, Arsiyanti A, Radji M. In Silico Molecular Docking Study of Gallic Acid and its Derivatives as Inhibitor BRAF Colon Cancer. *International Journal of ChemTech Research,* 2017,10(1): 310-315.
16. Patel BD, Ghate MD. 3D-QSAR studies of dipeptidyl peptidase-4 inhibitors using various alignment methods. *Med Chem Res* 2014;24:1060-9.
17. Wold S, Rhue A, Wold H, Dunn W. The collinearity problem in linear regression. The partial least squares approach to generalized inverses. *SIAM J Sci Stat Comput* 1984;5:735-43.
18. Cramer III RD, Bunce JD, Patterson DE, Frank IE. Crossvalidation, bootstrapping, and partial least squares compared with multiple regression in conventional QSAR studies. *Quantitative Structure-Activity Relationships.* 1988;7(1):18-25.
19. Vyas VK, Shah S, Ghate M. Generation of new leads as HIV-1 integrase inhibitors: 3D QSAR, docking and molecular dynamics simulation. *Medicinal Chemistry Research.* 2017 Mar 1;26(3):532-50.

\*\*\*\*\*